Fuel 358 (2024) 130129

Contents lists available at ScienceDirect

Fuel

journal homepage: www.elsevier.com/locate/fuel

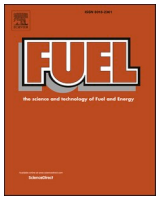

Full Length Article

Performance of SOFCs using model waste gases: A case study

E.V. Tsipis [a,*], D.V. Matveev [a], A.U. Sharafutdinov [a], D.V. Yalovenko [a], A.V. Samoilov [a], Yu.S. Fedotov [a], M.S. Dyakina [a], D.V. Zhigacheva [a], D.A. Agarkov [a,b], S.I. Bredikhin [a], V. V. Kharton [a]

[a] Osipyan Institute of Solid State Physics RAS, 2 Academician Osipyan Str., Chernogolovka, Moscow Distr., 142432, Russia
[b] Moscow Institute of Physics and Technology, 9 Institutskiy per., Dolgoprudny 141701, Russia

ARTICLE INFO

Keywords:
Solid oxide fuel cells
Waste gas utilization
Municipal solid waste landfill gas
Coke-oven gas
Methane conversion
Long-term operation

ABSTRACT

Municipal solid waste landfills and steelmaking industry produce large amounts of high-calorific waste gases which can be utilized for energy generation. The possibility of SOFC operation using model landfill and coke-oven gases without external steam reforming of methane was experimentally demonstrated employing a SOFC short-stack comprising two electrolyte-supported membrane-electrode assemblies of planar geometry. The current-voltage dependencies, polarization resistances and composition of the effluent fuel oxidation products were tested as function of time during approximately 600 h. In all cases, complete conversion of methane occurs at the anodes even under open-circuit conditions. The maximum power density of 183 mW/cm^2 was achieved for the humidified landfill gas at 850 °C and current density of 320 mA/cm^2; the fuel utilization was 67% at current density of 222 mA/cm^2. Neither microstructural changes nor carbon deposition were revealed by microscopic analyses after the SOFC tests. However, thermodynamic estimations showed that local anode coking may occur in a narrow zone near the fuel inlet where the fuel utilization only starts. This process correlating with local cooling detected in the vicinity of fuel inlet, may be responsible for degradation in the SOFC performance observed in the waste gas utilization regime.

1. Introduction

The ever-growing demand for new energy sources, increasing amount of municipal solid wastes (MSWs) and industrial emissions in the atmosphere become more and more acute every year. The calorific waste gases produced by industry and MSW landfills can be utilized to generate electrical and thermal energy, thus reducing environmental threats [1–15]. Furthermore, over 2 × 10^9 tons of municipal solid waste are globally generated every year and this amount tends to increase [16]. The MSW landfills should hence be considered as sources of biogas formed due to the organic waste decay. The main components of these gas mixtures are CH_4 and CO_2 ([3–5,9,17,18], Table 1). The generation rate and composition of the landfill biogas are however unstable, depending on the ambient temperature, humidity, atmospheric oxygen access, waste components and time period after the landfill operation start. The methane generation potential of MSWs may vary in a wide range from 35 up to 164 m^3/t [9,17]. The gases generated as by-products of steelmaking contain mainly CH_4, H_2 and CO [10,12–15]. In particular, the amount of globally produced coke-oven gas is estimated as 650 Mt/year; only ≤50% of this gas is re-utilized within the steelmaking processes [14]. The coke-oven gas consists mainly of hydrogen and methane (Table 1) and may be utilized for energy production.

Electric power and heat cam be generated using methane-containing waste gases in reciprocating internal combustion engines (ICEs), gas turbines (GTs), fuel cells or combinations of these technologies. The efficiency of fuel cells is substantially higher with respect to ICEs and GTs. In the case of molten carbonate fuel cells (MCFCs) and solid oxide fuel cells (SOFCs), mixtures of H_2 and CO are generated in the external converter or internally within the fuel cell stack due to the high operating temperatures, usually >500 °C. SOFCs possess a higher tolerance to CO and impurities compared to MCFCs. The low-temperature fuel cells such as phosphoric acid, alkaline and proton-exchange membrane fuel cells requiring a complex external fuel processor to produce high-purity H_2, are less suitable for the waste gas utilization. Although the gas combustion engines are currently more cost-efficient, the SOFC application is expedient from the environment point of view [19]. Important advantages of SOFCs include their high energy-conversion

* Corresponding author.
E-mail address: tsipis@issp.ac.ru (E.V. Tsipis).

https://doi.org/10.1016/j.fuel.2023.130129
Received 17 July 2023; Received in revised form 3 October 2023; Accepted 15 October 2023

Table 1
Main components of landfill and coke-oven gases.

Gas type	Composition, vol.%					Ref.
	CH_4	N_2	CO	CO_2	H_2	
Landfill	35–70	< 1–25	0–0.2	24–60	0–3	[3–5,9]
Coke oven	23–34	4–6	5–10	2–5	51–60	[10,12–14]

efficiency even at low scale, fuel flexibility, environmental safety, noiseless operation, and a possibility to recover exhaust heat. Recent developments in the SOFC systems include the use of natural gas [20], biogas [20,21], coal mine gas [22] and ammonia [23], with significant efforts directed towards decarbonization and emission reduction [24].

The SOFC-based technologies are considered as a feasible solution for the waste gas utilization problems [4–8,10–12]. However, literature data on the SOFC performance using methane-containing fuels are contradictory, and were often obtained on the button cells with a small electrode area. For instance, the small tubular SOFCs (total cathode area of 2.4 cm^2) operating on Cannock landfill gas after desulfurization reached the power output of approximately 170 mW at 850 °C; after the operation for 6 h, the performance decreased by ~30% [4]. The anode-supported microtubular SOFC operating on the landfill gas, produced from pilot-scale anaerobic bioreactors, showed a maximum power density of 0.11 W/cm^2 at 775 °C [25]. The planar electrolyte-supported SOFC demonstrated a maximum power density of about 80 mW/cm^2 in humidified (3% H_2O) CH_4 at 850 °C and a degradation rate of 0.08 mW/h at the current density of 180 mA/cm^2 [26]. The electrolyte-supported SOFC operating on humidified synthetic biogas (47% CH_4 - 47% CO_2 - H_2O) had a maximum power density of 210 W/cm^2 at 800 °C; the carbon deposition problems were acknowledged [27]. For the anode-supported SOFC where the anode comprised $La_{0.6}Sr_{0.2}Cr_{0.85}Ni_{0.15}O_3$ catalyst, a maximum power density of as high as 0.758 W/cm^2, methane conversion of 85.5% and stable operation were reported when using dry 50% CH_4 - 50% CO_2 fuel at 750 °C [28]. For the sake of comparison, the commercial electrolyte-supported SOFCs [29] provide a maximum fuel utilization of 47% at the operational voltage of 0.7 V and generate approximately 0.38 W/cm^2 at 800 °C using hydrogen fuel.

The present work was focused on the evaluation of electrolyte-supported planar SOFC performance using model landfill and coke-oven gases. The commercial-scale fuel cells were produced of conventional electrode and electrolyte materials. The short-stack of these cells was assembled and tested with a special attention to long-term stability.

2. Experimental

In order to study operational features of SOFCs utilizing waste gases, a short-stack with two membrane-electrode assemblies (MEAs) was produced; the design and processing techniques were reported elsewhere [30–32]. The solid electrolyte membrane represented a three-layer gas-tight plate (10 × 10 cm^2), consisting of one 90 μm thick

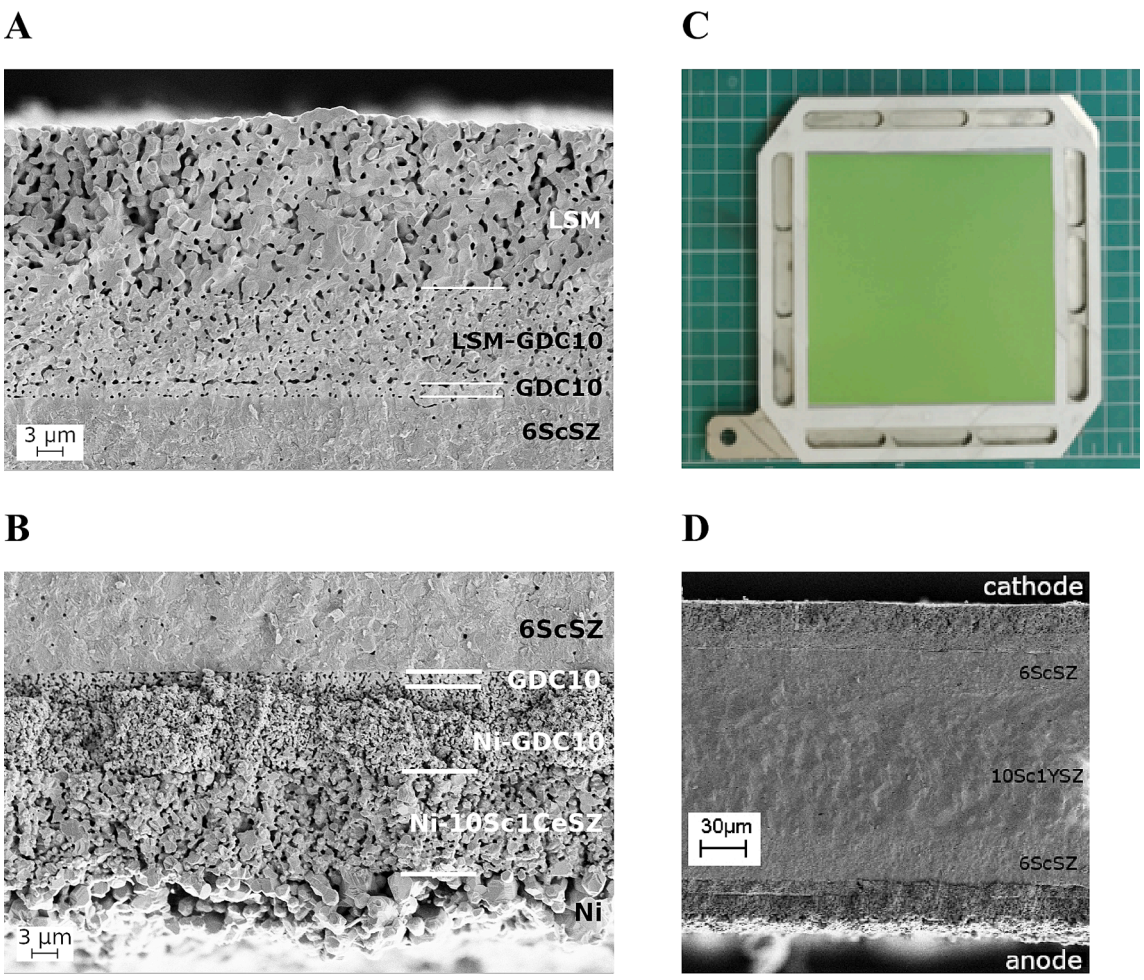

Fig. 1. SEM images of as-prepared MEA showing cathodic porous layer (A) consisting of (from top to bottom): LSM, LSM-GDC10 (60–40 wt%) composite and GDC10 layers, and anodic porous layer (B) consisting of NiO, NiO-10Sc1CeSZ (60–40 wt%) composite, NiO-GDC10 (50–50 wt%) composite and GDC10 deposited onto 6ScSZ. Photo of one stage of SOFC stack manufacturing (C). SEM micrograph of the fractured MEA consisting of a layered porous cathode, a three-layer gas-tight solid electrolyte and a layered porous anode, after SOFC tests using model waste gases (D).

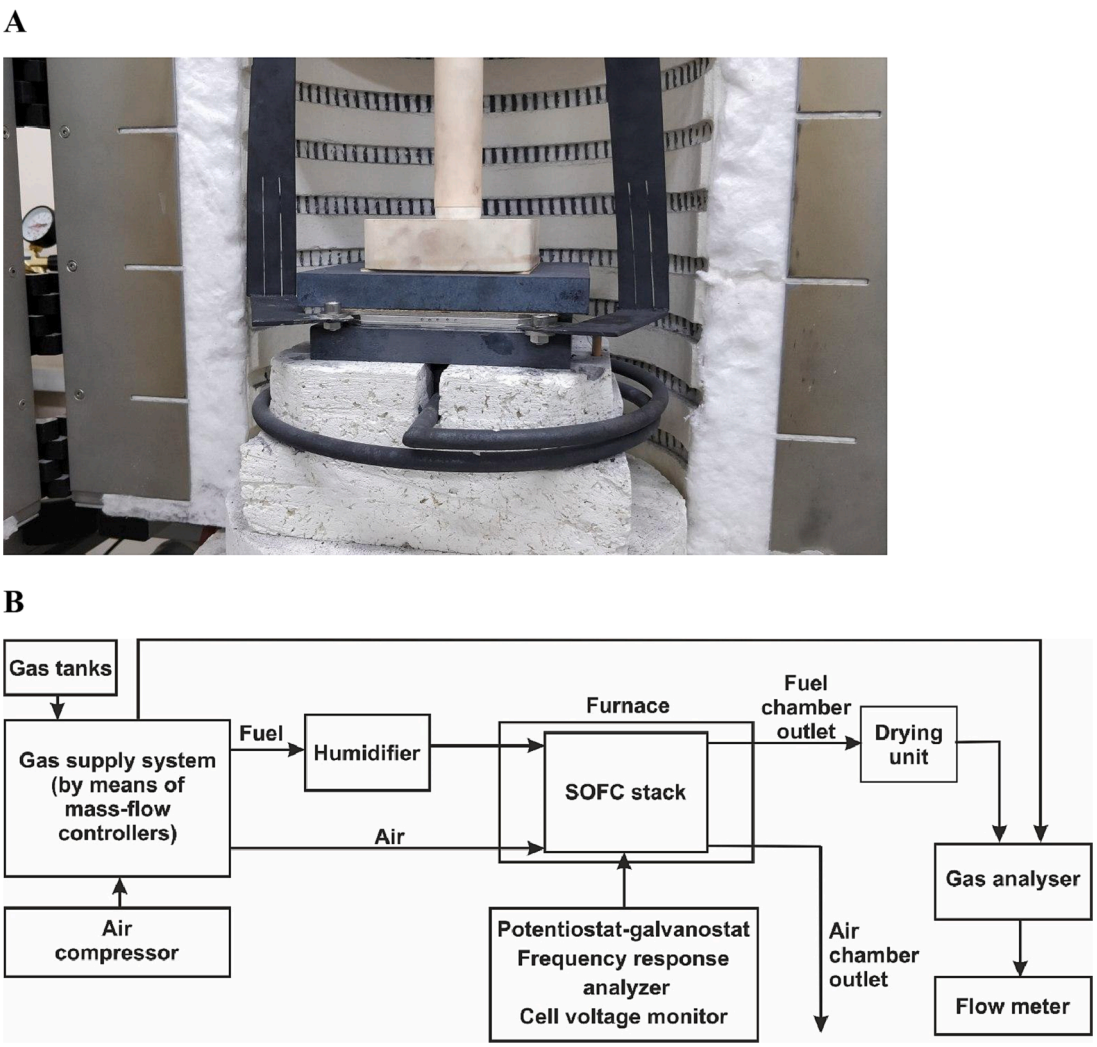

Fig. 2. Photo of the SOFC stack placed in the furnace (A), and schematic drawing of the experimental setup for SOFC testing (B).

internal layer of 10 mol.% Sc_2O_3 and 1 mol.% Y_2O_3 co-stabilized ZrO_2 (10Sc1YSZ) and two 30 μm thick external layers of 6 mol.% Sc_2O_3-stabilized ZrO_2 (6ScSZ) [33,34]. The electrode layers (geometric area of 9 × 9 cm^2) were applied by screen-printing using an EKRA E2 instrument (EKRA Innovative Technologien, Germany). The electrode pastes were prepared by mixing of ball-milled oxide powders with an organic binder. After screen-printing, the electrode layers were dried and finally co-sintered in air at 1300 °C. The porous cathodes comprised a protective interlayer of $Ce_{0.9}Gd_{0.1}O_{1.95}$ (GDC10) (thickness of 1.5 μm after sintering), composite $(La_{0.8}Sr_{0.2})_{0.95}MnO_{3-\delta}$ (LSM) - GDC10 (60–40 wt%, 10 μm) functional layer, and LSM (20 μm) current-collecting layer (Fig. 1A). The single-phase LSM powder was synthesized via the glycine-nitrate process [35]; all other powders were commercially available. The anode consisted of successive GDC10 (1.5 μm), NiO - GDC10 composite (50–50 wt%, 10 μm), NiO - 10Sc1CeSZ composite (60–40 wt%, 12 μm), and NiO (~5 μm) layers (Fig. 1B). The protective interlayers are necessary to prevent chemical interaction and interdiffusion between the electrode and electrolyte materials. The resulting electrodes had a good mechanical strength and a well-developed porous microstructure (Fig. 1). The current collectors were fabricated of Ni-coated Crofer 22H stainless steel [36–38]. The contact layers of LSM and NiO pastes were deposited on the current collectors or nickel mesh covering the anode layer, respectively. A commercially available glass-ceramic sealant (Kerafol, Germany) was used to hermetically seal the SOFC assembly. One of the stack fabrication steps is shown in Fig. 1C. After assembling, the short-stack was installed in a laboratory test setup Evaluator C1000-HT (Horiba FuelCon, Germany) under mechanical load of 0.2 kg/cm^2 (Fig. 2). The measurements were performed at 850 °C using a potentiostat-galvanostat/frequency-response analyzer (FRA) Reference 3000 (Gamry Instuments, USA) with a Reference 30 k booster. The gas supply rates were settled by mass-flow controllers (Bronkhorst Instruments, Germany). Atmospheric air (2500 ml/min) was supplied onto the cathodes; the mixtures of CH_4 - CO_2 or H_2 - CH_4 - CO - CO_2 were supplied into anode chambers at the total flow rates of 218 and 749 ml/min, respectively. The fuel gas mixtures were humidified at 65 °C (Fig. 2B). In order to study the composition of gaseous products formed in the SOFC anode chamber, a gas analysis system was assembled employing Ultramat 23 and Calomat 6 gas analyzers (Siemens, Germany) and a Test-1 analyzer (Boner, Russia). The scanning electron microscopy coupled with energy dispersive spectroscopy (SEM/EDS) employing a Supra 50VP microscope (CarlZeiss, Germany) equipped by INCA detector (Oxford Instruments, UK) was used for the microstructural analysis before and after the stack testing. Surface mapping was carried out under standard conditions with an accelerating voltage of 20 kV. The spectrum acquisition time was >120 min. Separately, a series of EDS tests were carried out from different places of the anode surface at an accelerating voltage of 10 kV, which makes it possible to register lighter elements with a higher accuracy.

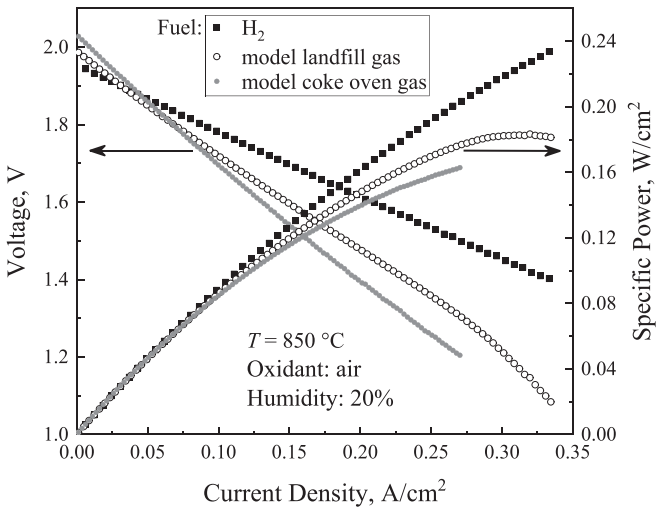

Fig. 3. Comparison of the current-voltage curves and power density of the two-MEA SOFC stack operating at 850 °C using 80 %H_2 - 20 % H_2O and mixtures simulating landfill (36.2 % CH_4 - 43.8 % CO_2 - 20 % H_2O) and coke oven (45.6 % H_2 - 20.8 % CH_4 - 5.1 % CO - 8.5 % CO_2 - 20 % H_2O) gases.

3. Results and discussion

3.1. Selection of the MEA design and operating conditions: A brief justification

The choice of SOFC design depends on many factors including the application type, planned fuels, load profile over time and other requirements to the power plant. In turn, this choice largely determines the SOFC stack operation conditions, such as temperature and fuel preprocessing. Currently, there exist three most common approaches for the design of planar SOFCs: electrolyte-supported cells (so-called 1st generation SOFCs), electrode-supported cells (2nd generation), and the cells with external support of porous metal or ceramics (3rd generation) [39,40]. These all have specific advantages and disadvantages. The high operating temperature of such SOFCs (800–900 °C) enables internal conversion of hydrocarbons and reduces the carbon deposition problem [27]. On the other hand, the relatively thick electrolyte determines up to a half of total internal resistance of the cell, thus increasing ohmic losses and decreasing power density. Furthermore, the high operation temperatures may be associated with accelerated microstructural degradation and severe restrictions on the selection of construction materials, such as stainless steel for the current collectors/interconnectors.

The 2nd and 3rd generation SOFCs require the use of solid electrolyte membranes with thickness up to 5 μm, which decreases ohmic losses; in this case, the output power density becomes substantially higher. Lowering of the operating temperature down to the so-called intermediate range, 600–750 °C, expands the spectrum of materials which can be employed for current collection and hermitization. However, the use of thin-film technologies increases the SOFC manufacturing costs and may have a negative impact on the cell reliability during long-term operation, especially in terms of the electrolyte/electrode interface stability. The decrease in operating temperature hampers internal conversion of hydrocarbon fuels and promotes carbon deposition at the anode. Therefore, planar SOFCs with supporting electrolyte membranes were used in the present work centered on the utilization of methane-containing waste gases.

The SOFC operating temperature of 850 °C was chosen to provide a sufficiently fast kinetics of internal methane reforming and to decrease probability of anode coking with respect to the intermediate-temperature range. Taking into account the high-temperature corrosion of and interdiffusion between the stack components, such as glass-ceramic sealants and stainless-steel bipolar plates, this operation temperature could not be increased to a significant extent. The fuel mixture compositions tested in this work were selected as average in the ranges typical for the real waste gases (Table 1). Before humidification, the model landfill gas contained 45% CH_4 and 55% CO_2; the model coke-oven gas contained 57% H_2, 26% CH_4 and 6% CO. The steam concentration of 20% in the fuel was chosen as the value yielding gas-mixture composition close to the carbon deposition boundary, as discussed below. This level of humidification makes it possible to test SOFC durability under conditions when the anode coking risks are high enough.

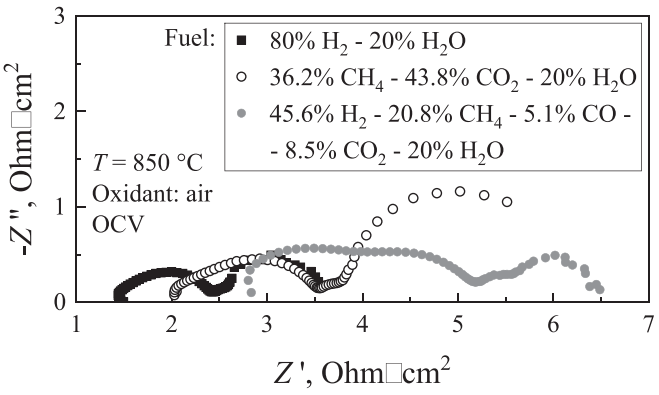

Fig. 4. Impedance spectra of two MEAs (total geometric area of 162 cm^2) fueled by 80 % H_2 – 20 % H_2O and model landfill and coke-oven gases at 850 °C under open-circuit conditions.

3.2. Utilization of model landfill and coke-oven gases in SOFCs

Fig. 3 compares the current-voltage curves and power densities of the 2 MEA-stack fueled by humidified hydrogen and model waste gases, namely landfill gas (36.2 % CH_4 - 43.8 % CO_2 - 20 % H_2O) and coke-oven gas (45.6 % H_2 - 20.8 % CH_4 - 5.1 % CO - 8.5 % CO_2 - 20 % H_2O) at 850 °C. The open-circuit voltage (OCV) values are in accordance with theoretical calculations. The OCV values per single MEA, calculated assuming instant conversion of methane at the fuel entry, are 0.954 V for 80% H_2 - 20% H_2O, 0.965 V for the landfill gas and 1.024 V for the coke-oven gas. The levels of SOFC performance obtained for the landfill and coke-oven gases are similar to one another and are worse than that for hydrogen fuel. This behavior agrees well with the literature data (e.g. [27,41] and references therein). At the current density of 320 mA/cm^2, the power is approximately 183 and 227 mW/cm^2 for the model landfill gas and 80 % H_2 - 20 % H_2O, respectively. In the former case, this value corresponds to maximum; at current densities above 275 mA/cm^2 the voltage losses related to the concentration polarization become significant. In the case of hydrogen fuel, the current-voltage dependence remains linear under the experimental conditions used in this work. The activation polarization is also much higher in the case of model waste gases with respect to hydrogen.

Fig. 4 displays the impedance spectra of two MEAs when using humidified pure H_2 and model waste gases under open-circuit conditions at 850 °C. The spectra consist of four resolvable arcs. Both ohmic and polarization losses increase after switching hydrogen to the CH_4-containing waste gases. The processes occurring at the SOFC electrodes make a larger contribution to the total internal resistance compared to the ohmic losses. One should also mention that both charge-transfer and diffusion processes, attributed usually to the high- and low-frequency signals, respectively, contribute to the increase of total electrode polarization resistance after the change of fuels. The diffusion contribution to the polarization resistance for the model coke oven gas containing H_2 is close to that observed for hydrogen fuel, whilst the contribution of the high-frequency component of the impedance spectrum is much higher than that for hydrogen. The diffusion limitations to the overall electrode

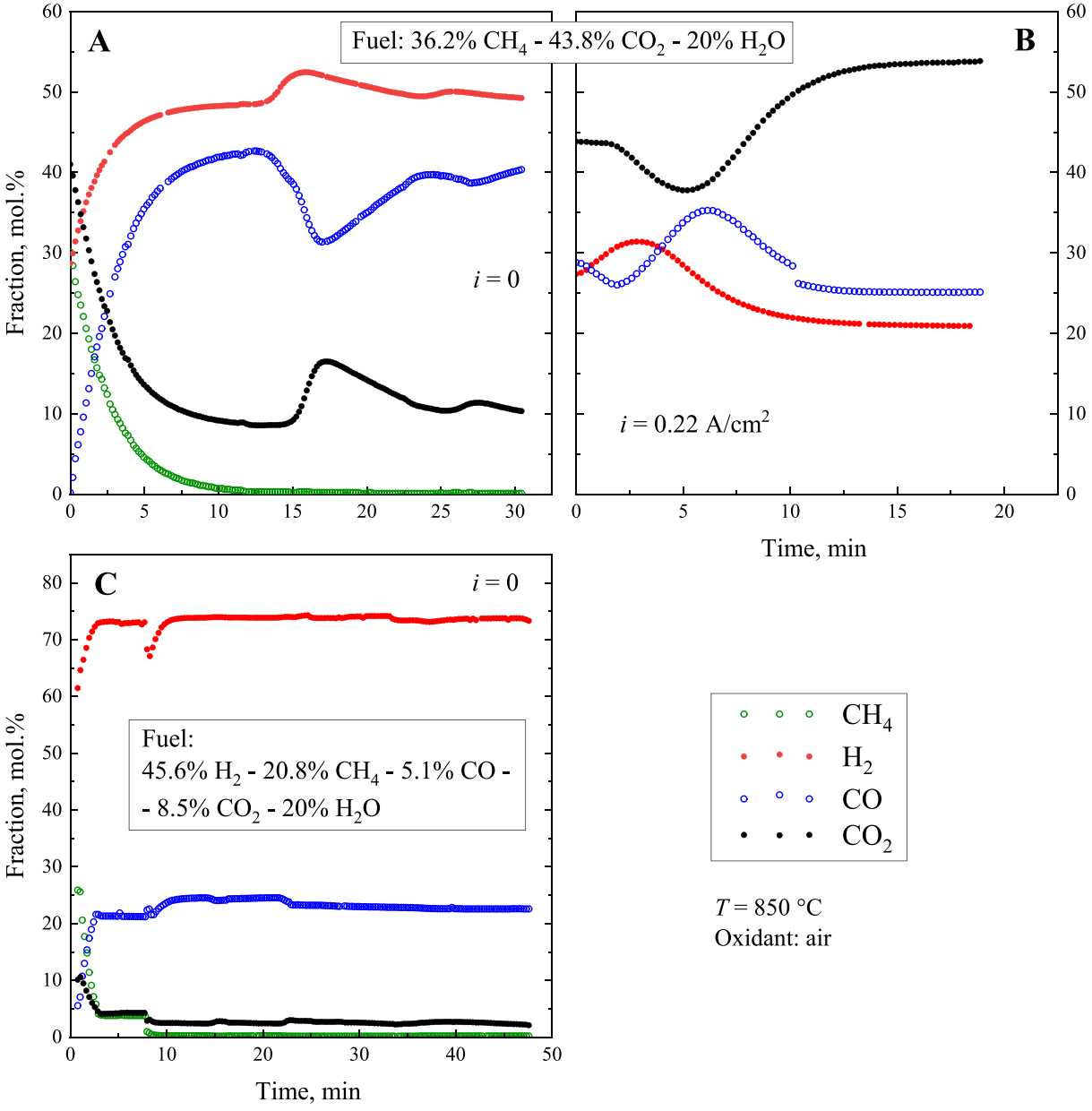

Fig. 5. Time dependences of the concentrations of anodic oxidation products recorded for the model landfill (A and B) and coke-oven (C) gases as fuels at 850 °C under open-circuit conditions (A and C) and under the current load of 18 A (B).

Table 2
Measured fluxes of C-containing components of the model landfill gas and their anodic oxidation products at 850 °C and various current loads, carbon balance and fuel utilization.

Gas	Flux, ml/min				
	Inlet	Outlet, 0 A	Outlet, 10 A	Outlet, 15 A	Outlet, 18 A
CH_4	98.5	0	0	0	0
H_2	0	208.0	122.8	79.8	56.6
CO_2	119.3	42.7	94.4	129.7	145.8
CO	0	168.0	116.4	83.3	68.1
ΣC	217.8	210.7	210.8	213.0	213.9
C imbalance, %		3.3	3.2	2.2	1.8
Fuel utilization, %			36.4	56.6	66.8

reaction are highest for the model landfill gas.

In order to assess the mechanism of fuel oxidation in the course of SOFC operation using CH_4-containing waste gases, the composition of the effluent gas mixtures was analyzed in real time under open-circuit conditions and under a load of 10, 15 and 18 A at 850 °C in combination with total effluent flow rate measurements. Selected data are presented in Fig. 5 and Table 2. In all cases, a complete conversion of methane occurs at the anode. When current load is applied, the fraction of hydrogen consumed at the anode is larger than that of CO; the total fuel utilization also increases with increasing current density, as expected.

Fig. 6 shows the voltage vs. time dependence at the currents of 18 and 10 A in model waste gases. Over a period of time longer than 360 h, voltage of the stack operating on landfill gas decreased by approximately 5%. This degradation rate is much higher than the targeted value, 0.2% per 1000 h. When the voltage reached 1.4 V, the current load was reduced down to 10 A and the life tests were continued. A

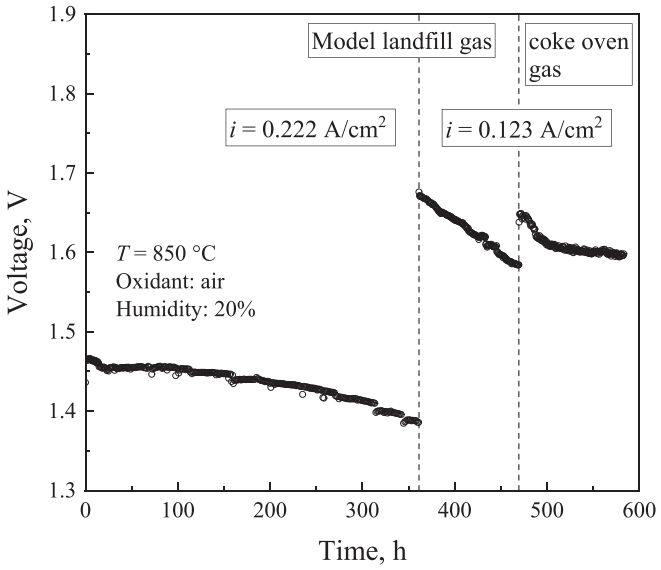

Fig. 6. Time dependence of voltage for the two-MEA SOFC stack operating on model landfill (36.2 % CH_4 - 43.8 % CO_2 - 20 % H_2O) and coke oven (45.6 % H_2 - 20.8 % CH_4 - 5.1 % CO - 8.5 % CO_2 – 20 % H_2O) gases at 850 °C and current loads of 10–18 A (123–222 mA/cm^2).

substantially large performance degradation was observed for the next 110 h (Fig. 6). When using the model coke-oven gas as a fuel, the voltage was also lower compared to pure hydrogen; the degradation occurs, however, much slower compared to the landfill gas. After testing and disassembling of the SOFC short stack, MEAs were fractured, and their cross-sections and surfaces were examined by SEM/EDS (Fig. 1D). The results show that, after the operation on model waste gases during almost 600 h, no significant microstructural changes appear. In particular, neither electrode delamination nor traces of carbon deposits were detected at the anode surface (Fig. 7). In order to identify processes relevant for the SOFC performance degradation, the calculated gas compositions along the fuel channel were analyzed with respect to the iso-activity lines corresponding to the unit chemical activity of solid carbon ($a_C = 1$).

3.3. Appraisal of the carbon deposition role

Fig. 8 compares the thermodynamic boundaries of carbon deposition [42] and the calculated evolution of gas compositions when the fuel utilization varies from 0 up to 100% at 850 °C, shown in the C - H - O coordinates. The calculations were performed using the NIST thermochemical data. It should be mentioned that, at elevated temperatures (above 600 °C), formation of the single-walled carbon nanotubes (SWCNT) is energetically favorable with respect to graphite [42]. For the tested fuel compositions, appearance of carbon nanotubes is possible under OCV conditions even at 850 °C, or at the very beginning of the fuel path under current load (Fig. 8). A local decrease of temperature, approximately 20 °C, was indeed experimentally detected in the vicinity

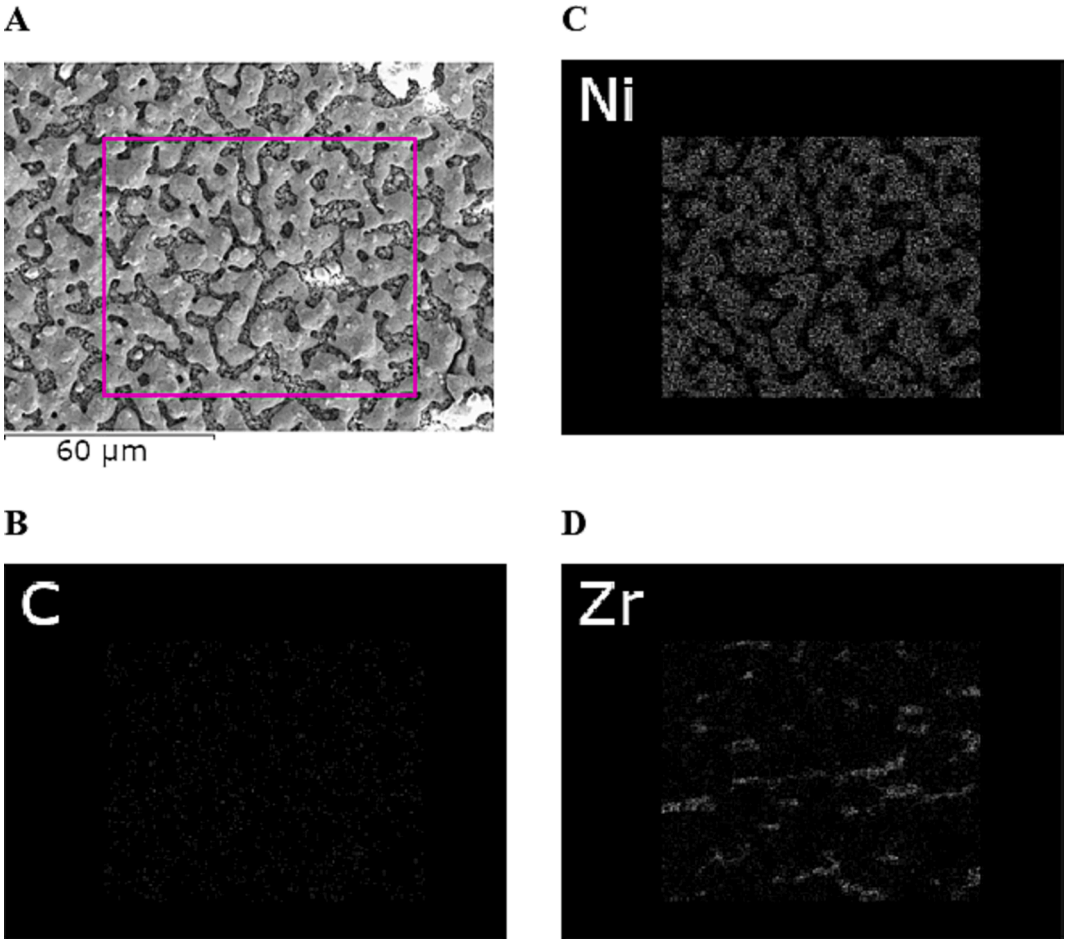

Fig. 7. SEM image (A) and the corresponding element distribution maps for carbon (B), nickel (C) and zirconium (D) for the anode surface after testing in model waste gases. The signal accumulation time was >2 h.

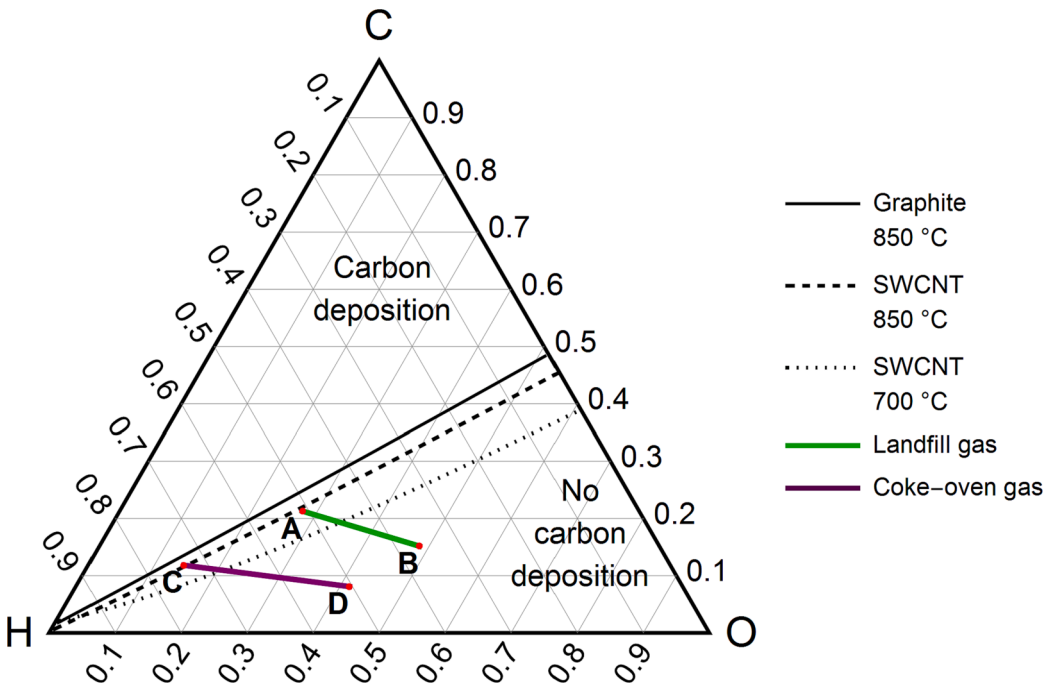

Fig. 8. C - H - O ternary diagram showing the evolution of effluent gas compositions when fuel utilization varies from 0 to 100% (thick purple and green lines) and iso-activity lines corresponding to the unit chemical activity of solid carbon ($a_C = 1$) [42] for different forms of carbon deposits at atmospheric total pressure. The red points A and C correspond to 0% fuel utilization; the points B и D correspond to 100% fuel utilization. SWCNT denotes single-walled carbon nanotubes. (For interpretation of the references to colour in this figure legend, the reader is referred to the web version of this article.)

of fuel inlet. This local cooling, which may also promote carbon deposition, is associated with the prevailing contribution of endothermic steam reforming of methane. At larger distances from the fuel inlet, temperature increases due to increasing roles of exothermic hydrogen oxidation and water-gas shift reactions. Increasing total current through the MEAs leads to carbon oxidation and increases fuel utilization (Table 2), resulting in a slower performance degradation (Fig. 6). These conclusions are in agreement with the results of SOFC modelling [43]. Since SEM/EDS analyses did not reveal carbon traces over most of the anode surface, coking should be essentially limited to a relatively narrow zone near the fuel inlet. The total carbon imbalance between the influent and effluent gas mixtures (Table 2) is approximately 3% under OCV conditions and decreases with increasing current density. Such small amounts of carbon may be removed, for example, by applying a H_2/H_2O regeneration gas mixture as suggested in Ref.[44]. At the same time, the interdiffusion processes at the cathode/electrolyte and electrode/interconnector interfaces, known to deteriorate SOFC performance, cannot be entirely excluded. The contact resistances may also depend on the fuel composition; in particular, the anode current collector/ interconnector contact may undergo degradation.

In summary, the results clearly demonstrated feasibility of long-term SOFC operation using waste gases as a fuel without external methane conversion. Optimization of the electrodes and experimental conditions, including temperature, humidity and gas flow rates, is however necessary to further improve the performance and durability of the SOFC stacks utilizing waste gases. The negative impact of local anode coking may be suppressed by increasing the steam/methane ratio in the influent gases, but any significant increase in the humidity level should unavoidably reduce power density. Developments of novel anode materials and catalysts active towards carbon oxidation are, therefore, necessary as the conventional SOFC anodes exhibit rather insufficient performance when utilizing waste gases.

4. Conclusions

The possibility of SOFC operation using landfill and coke-oven gases without external steam reforming of methane was experimentally demonstrated. The SOFC stack of two planar electrolyte-supported membrane-electrode assemblies was produced and tested at 850 °C using humidified model waste gases, namely landfill gas (36.2 % CH_4 - 43.8 % CO_2 - 20 % H_2O) and coke-oven gas (45.6 % H_2 - 20.8 % CH_4 - 5.1 % CO - 8.5 % CO_2 - 20 % H_2O). The performance of SOFC stack fueled by the model waste gases is worse compared to hydrogen fuel due to the higher ohmic and electrode polarization losses. In the case of landfill gas, the maximum power density of 183 mW/cm^2 was obtained at the current density of 320 mA/cm^2. In all cases, complete conversion of methane occurs at the anodes. Despite an apparent absence of carbon deposits visible for SEM/EDS analyses at the anode surface after the operation using methane-containing fuels for 584 h, a degradation in the SOFC performance was observed under testing conditions. Thermodynamic estimations showed that this degradation may be associated with local anode coking in the vicinity of fuel inlet, in agreement with local cooling detected in this narrow zone and minor carbon imbalance between the influent and effluent gas mixtures.

CRediT authorship contribution statement

E.V. Tsipis: Writing – original draft, Investigation, Data curation, Conceptualization. **D.V. Matveev:** Investigation, Data curation. **A.U. Sharafutdinov:** Writing – review & editing, Validation, Methodology, Investigation. **D.V. Yalovenko:** Investigation. **A.V. Samoilov:** Methodology, Investigation. **Yu.S. Fedotov:** Methodology, Investigation. **M. S. Dyakina:** Investigation. **D.V. Zhigacheva:** Investigation. **D.A. Agarkov:** Writing – review & editing, Visualization. **S.I. Bredikhin:** Supervision, Conceptualization. **V.V. Kharton:** Writing – review & editing, Supervision, Methodology, Conceptualization.

Declaration of Competing Interest

The authors declare that they have no known competing financial interests or personal relationships that could have appeared to influence the work reported in this paper.

Data availability

Data will be made available on request.

Acknowledgments

This work was supported by the Russian Science Foundation (grant 20-19-00478). The authors are sincerely grateful to I.A. Karpova for assistance in the SOFC stack assembling.

References

[1] Siwal SS, Zhang Q, Devi N, Saini AK, Saini V, Pareek B, et al. Recovery processes of sustainable energy using different biomass and wastes. Renew Sustain Energy Rev 2021;150:111483.
[2] Mukherjee C, Denney J, Mbonimpa EG, Slagley J, Bhowmik R. A review on municipal solid waste-to-energy trends in the USA. Renew Sustain Energy Rev 2020;119:109512.
[3] Lombardi L, Carnevale E, Corti A. Greenhouse effect reduction and energy recovery from waste landfill. Energy 2006;31:3208–19.
[4] Staniforth J, Kendall K. Cannock landfill gas powering a small tubular solid oxide fuel cell — a case study. J Power Sources 2000;86:401–3.
[5] Papurello D, Silvestri S, Tomasi L, Belcari I, Biasioli F, Santarelli M. Biowaste for SOFCs Energy Proc 2016;101:424–31.
[6] Abdelkareem MA, Tanveer WH, Sayed ET, El Haj AM, Allagui A, Cha SW. On the technical challenges affecting the performance of direct internal reforming biogas solid oxide fuel cells. Renew Sust Energy Rev 2019;101:361–75.
[7] Kiseleva S, Tarasenko A, Shakun V, Agarkov D. Hydrogen energy in Russia – industrial waste gases utilization potential. J Phys: Conf Ser 2021;1960:012010.
[8] Agarkov DA, Bredikhin SI, Kiseleva SV, Matveev DV, Samoilov AV, Tarasenko AB, et al. Solid oxide fuel cells' prospects for landfill gas utilization in Russia. Therm Eng 2023;70:72–8.
[9] Aguilar-Virgen Q, Taboada-González P, Ojeda-Benítez S, Cruz-Sotelo S. Power generation with biogas from municipal solid waste: Prediction of gas generation with in situ parameters. Renew Sustain Energy Rev 2014;30:412–9.
[10] Liu W, Sang J, Wang Y, Chang X, Lu L, Wang J, et al. Durability of direct-internally reformed simulated coke oven gas in an anode-supported planar solid oxide fuel cell based on double-sided cathodes. J Power Sources 2020;465:228284.
[11] Xiang D, Huang W, Cai M, Cao Y, Li P, Shu R. Process modeling, simulation, and technical analysis of coke-oven gas solid oxide fuel cell integrated with anode off-gas recirculation and CLC for power generation. Energy Convers Manag 2019;190:34–41.
[12] Zhao H, Jiang T, Hou H. Performance analysis of the SOFC-CCHP system based on H_2O/Li-Br absorption refrigeration cycle fueled by coke oven gas. Energy 2015;91:983–93.
[13] Yang Y, Raipala K, Holappa L. Ironmaking. Treatise on. Process Metallurgy 2014;3:2–88.
[14] Czachor M, Laycock CJ, Carr SJW, Maddy J, Lloyd G, Guwy AJ. Co-electrolysis of simulated coke oven gas using solid oxide electrolysis technology. Energy Convers Manag 2020;225:113455.
[15] Musial D, Szwaja M, Kurtyka M, Szwaja S. Usage of converter gas as a substitute fuel for a tunnel furnace in steelworks. Mater 2022;15:5054.
[16] Website of the World Bank, https://datatopics.worldbank.org/what-a-waste/trends_in_solid_waste_management.html [assessed 1 April 2023].
[17] Chickering GW, Krause MJ, Townsend TG. Determination of as-discarded methane potential in residential and commercial municipal solid waste. Waste Manag 2018;76:82–9.
[18] Allen MR, Braithwaite A, Hills CC. Trace organic compounds in landfill gas at seven U.K. waste disposal sites. Environ Sci Technol 1997;31(4):1054–61.
[19] Kistner L, Schubert FL, Minke Ch, Bensmann A, Hanke-Rauschenbach R. Techno-economic and environmental comparison of internal combustion engines and Solid Oxide Fuel Cells for ship applications. J Power Sources 2021;508:230328.
[20] SO-FREE project website, https://www.so-free.eu [Accessed 5 September 2023].
[21] WASTE2WATTS (W2W) website, https://waste2watts-project.net [Accessed 5 September 2023].
[22] Groß B, Blum L, de Haart LGJ, Dengel A. Development of a Solid Oxide Fuel Cell for the utilization of coal mine gas. J Power Sources 2011;196:5309–16.
[23] ShipFC project website, https://shipfc.eu/about [Accessed 5 September 2023].
[24] HELENUS project website, https://www.helenus.eu [Accessed 5 September 2023].
[25] Yaman C, Kucukaga Y. Performance of NiO/YSZ anode-supported solid oxide fuel cell fueled with landfill gas stream. E3S Web Conf 2020;166:04007.
[26] Escudero MJ, Yeste MP, Cauqui MÁ, Muñoz MÁ. Performance of a direct methane Solid Oxide Fuel Cell using nickel-ceria-yttria stabilized zirconia as the anode. Materials (Basel) 2020;13(3):599.
[27] Girona K, Laurencin J, Fouletier J, Lefebvre-Joud F. Carbon deposition in CH4/CO2 operated SOFC: Simulation and experimentation studies. J Power Sources 2012;210:381–91.
[28] Wei T, Qiu P, Yang J, Jia L, Chi B, Pu J, et al. High-performance direct carbon dioxide-methane solid oxide fuel cell with a structure-engineered double-layer anode. J Power Sources 2021;484:229199.
[29] fuelcellmaterials web-site, https://fuelcellmaterials.com/nextcell-versus-nextcell-hp-comparing-performance-data [Accessed 5 September 2023].
[30] Agarkova EA, Matveev DV, Fedotov YS, Ivanov AI, Agarkov DA, Bredihin SI. Processing of manganite-based contact layers for stacking of planar solid oxide fuel cells. Mat Lett 2022;309:131462.
[31] Matveev DV, Fedotov YS, Ivanov AI, Agarkova EA, Bredikhin SI. Optimization of Contact Cathode Composition Based on La0.8Sr0.2MnO3±δ for SOFC Stacks. ECS Trans 2021;103(1):1453–60.
[32] Burmistrov IN, Agarkov DA, Korovkin EV, Yalovenko DV, Bredikhin SI. Fabrication of Membrane-Electrode Assemblies for Solid-Oxide Fuel Cells by Joint Sintering of Electrodes at High Temperature. Russ J Electrochem 2017;53(8):873–9.
[33] Agarkova EA, Agarkov DA, Burmistrov IN, Zadorozhnaya OY, Yalovenko DV, Nepochatov YK, et al. Three-layered membranes for planar solid oxide fuel cells of the electrolyte-supported design: characteristics and applications. Russ J Electrochem 2020;56(2):132–8.
[34] Zadorozhnaya OY, Agarkova EA, Tiunova OV, Nepochatov YK. Layered solid-electrolyte membranes based on zirconia: production technology. Russ J Electrochem 2020;56(2):124–31.
[35] Chick LA, Pederson LR, Maupin GD, Bates JL, Thomas LE, Exarhos GJ. Glycine-nitrate combustion synthesis of oxide ceramic powders. Mater Lett 1990;10(1–2):6–12.
[36] Pikalov OV, Matveev DV, Levin MN, Demeneva NV. Features of oxidation of ferritic chromium steels as materials for current collectors of solid oxide fuel cells. Chernye Metally 2020;10:10–5.
[37] Demeneva NV, Kononenko OV, Matveev DV, Kharton VV, Bredikhin SI. Composition-gradient protective coatings for solid oxide fuel cell interconnectors. Mat Lett 2019;240:201–4.
[38] Demeneva NV, Matveev DV, Kharton VV, Bredikhin SI. Regularities of high-temperature oxidation of current collectors of solid oxide fuel cells due to diffusion processes in subsurface regions. Russ J Electrochem 2016;52(7):678–84.
[39] Cooper SJ, Brandon NP. An introduction to Solid Oxide Fuel Cell materials, technology and applications. In: Brandon NP, Ruiz-Trejo E, Boldrin P, editors. Solid Oxide Fuel Cell Lifetime and Reliability. Academic Press; 2017. p. 1–18. ISBN 9780081011027.
[40] Mendonça C, Ferreira A, Santos D. Towards the commercialization of Solid Oxide Fuel Cells: Recent advances in materials and integration strategies. Fuels 2021;2:393–419.
[41] Tsipis EV, Kharton VV. Electrode materials and reaction mechanisms in solid oxide fuel cells: a brief review. III. Recent trends and selected methodological aspects. J Solid State Electrochem 2011;15:1007–40.
[42] Jaworski Z, Zakrzewska B, Pianko-Oprych P. On thermodynamic equilibrium of carbon deposition from gaseous C-H-O mixtures: updating for nanotubes. Rev Chem Eng 2017;33:217–35.
[43] Aguiar P, Adjiman CS, Brandon NP. Anode-supported intermediate-temperature direct internal reforming solid oxide fuel cell: II. Model-based dynamic performance and control. J Power Sources 2005;147:136–47.
[44] Pongratz G, Subotić V, von Berg L, Schroettner H, Hochenauer C, Martini S, et al. Real coupling of solid oxide fuel cells with a biomass steam gasifier: Operating boundaries considering performance, tar and carbon deposition analyses. Fuel 2022;316:123310.